

# Infrared Spectroscopy of Intramolecular Hydrogen-Bonded OH Stretching Vibrations in Jet-Cooled Methyl Salicylate and Its Clusters

Akira Mitsuzuka, Asuka Fujii,\* Takayuki Ebata, and Naohiko Mikami\*

Department of Chemistry, Graduate School of Science, Tohoku University, Sendai 980-8578, Japan

Received: July 21, 1998; In Final Form: September 23, 1998

The OH stretching vibration of methyl salicylate and its solvated clusters in a supersonic free jet was observed by using fluorescence-detected infrared spectroscopy. The OH band of methyl salicylate monomer was weak and broad because of the intramolecular hydrogen bond. Those of the methyl salicylate moiety in small size hydrogen-bonded clusters with various solvent molecules, such as methyl salicylate-(H<sub>2</sub>O)<sub>n</sub> (*n* = 1 and 2), -CH<sub>3</sub>OH, and -NH<sub>3</sub>, also showed similar characteristics, indicating that the intramolecular hydrogen bond is retained even in the clusters. The opposite behavior of the direction of the electronic transition frequency shift and the OH stretching frequency shift was seen between the clusters with the acidic (water and methanol) and basic (ammonia) solvents. Structures for these clusters are discussed on the basis of the frequency shifts of the OH bond.

## Introduction

Methyl salicylate (MS) is a typical molecule having an intramolecular hydrogen bond between its hydroxyl and carbonyl groups. Excited-state intramolecular proton transfer (ESIPT) along this bond has been well-known from studies on the Stokes shift in the fluorescence spectrum.<sup>1–6</sup> Since MS in the electronically ground state, S<sub>0</sub>, is a weak acid (pK<sub>a</sub> = 10.2),<sup>7</sup> it enables to donate a proton to solvent in a solution. These features of the free molecule are contrary to those in the solution; therefore, a breakdown of the intramolecular hydrogen bond and formation of intermolecular hydrogen bonds may be expected along with the transformation from a monomer to a solution.

Such a transformation would be observed as the size dependence of infrared (IR) spectra of the hydrogen-bonded clusters. It has been well-known that IR absorption intensity and frequency of OH stretching vibrations show a drastic change due to the hydrogen-bond formation. The intermolecular hydrogen-bond formation leads to a remarkable enhancement in absorption intensity and to a reduction in OH vibrational frequency. On the other hand, an OH band involving an intramolecular hydrogen bond tends to be weak in intensity though the frequency is largely reduced. Recently, infrared spectroscopy has been applied to jet-cooled molecules and clusters having an intramolecular hydrogen bond, namely, tropolone and its hydrogen-bonded clusters.<sup>8–10</sup> The OH stretching vibration of tropolone showed a sudden change in intensity and a remarkable frequency shift when the cluster size exceeds a critical size. This change was interpreted as evidence of the transformation from the intramolecular to intermolecular hydrogen bond.<sup>8</sup>

MS is also an intramolecular hydrogen-bonded molecule; however, the acidity of MS is much smaller than that of tropolone (pK<sub>a</sub> = 6.7).<sup>11</sup> Therefore, microsolvation of MS is expected to show a different behavior from tropolone. In this paper, we observed IR spectra of bare MS and its hydrogen-bonded clusters with several solvents in the OH stretch region, and effects of the microsolvation are discussed.

## Experimental Section

We utilized fluorescence-detected infrared spectroscopy (FDIRS) to measure IR spectra of bare molecules and clusters in supersonic jets. The experimental apparatus for FDIRS has been described in detail elsewhere,<sup>8,12</sup> so that only a brief description is given here. A pulsed ultraviolet (UV) laser beam of which wavelength was fixed at the S<sub>1</sub>-S<sub>0</sub> transition was introduced, and the laser-induced fluorescence signal was detected as a measure of the population in the S<sub>0</sub> state. A pulsed IR beam was introduced 50 ns prior to the UV laser, and its wavelength was scanned. When the IR laser frequency is resonant with a vibrational transition in the ground state, decrease of the ground-state population results in a reduction (dip) of the fluorescence intensity from the S<sub>1</sub> state. Thus, by scanning the IR laser wavelength, fluorescence dip spectra that correspond to infrared absorption spectra of the ground state were obtained. Species and size selection in the spectrum measurement is performed by selecting the UV laser wavelength.

The tunable IR beam was obtained by a difference frequency generation with a LiNbO<sub>3</sub> crystal, in which a second harmonic of a Nd:YAG laser (Quanta-Ray GCR230) and an output of a Nd:YAG laser pumped dye laser (LAS LDL20505) were mixed. The UV light source was a second harmonic of a XeCl excimer laser pumped dye laser (Lambda Physik LPX100/FL3002). Temporal pulse widths of both lasers were about 8 ns. Accuracy of the laser frequencies were about 0.5 cm<sup>-1</sup>. The IR beam, focused at 10 mm downstream of a pulsed jet nozzle by a lens (*f* = 250 mm), was counterpropagated to the UV laser beam which was focused by a lens of *f* = 500 mm.

The MS sample was purchased from Tokyo Kasei Co. and was used without further purification. The MS vapor at room temperature was seeded in helium (stagnation pressure of 3 atm) containing solvent vapor and was expanded supersonically into a vacuum chamber through a pulsed nozzle with an orifice of 0.8 mm diameter.

## Results

**Electronic Spectra of MS and Its Hydrogen-Bonded Clusters.** The fluorescence excitation spectrum of the S<sub>1</sub>-S<sub>0</sub>

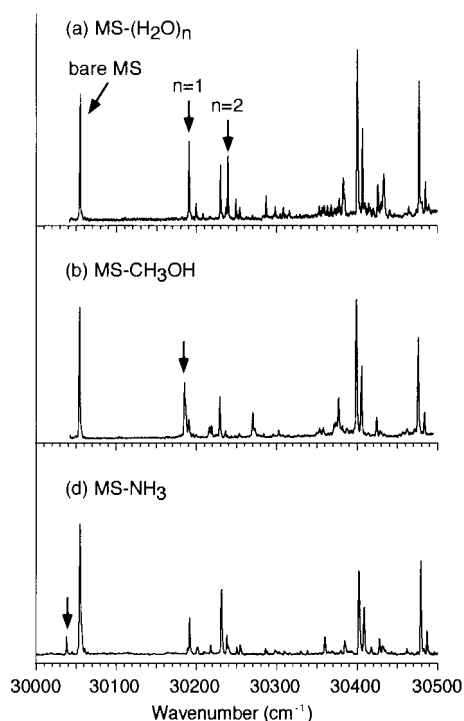


**Figure 1.** Fluorescence excitation spectra of the  $S_1-S_0$  transitions of (a) methyl salicylate (MS)– $(H_2O)_n$  ( $n = 1$  and  $2$ ), (b) MS– $CH_3OH$ , and (c) MS– $NH_3$  hydrogen-bonded clusters. The arrows indicate the band origins of the clusters.

**TABLE 1:  $S_1-S_0$  Transition Energies of Methyl Salicylate (MS) and Its Hydrogen-Bonded Clusters**

	band origin/ $cm^{-1}$	$\Delta\nu/cm^{-1}$
MS	30 055	
MS– $H_2O$	30 192	+137
MS– $(H_2O)_2$	30 241	+186
MS– $CH_3OH$	30 186	+131
MS– $NH_3$	30 038	–17

transitions of MS and MS– $(H_2O)_n$  ( $n = 1$  and  $2$ ) clusters is shown in Figure 1a. The observed electronic spectrum is essentially the same as that reported by Helmbrook and co-workers,<sup>3</sup> except for the presence of the water cluster bands. The 0–0 band of MS monomer occurs at  $30\,055\,cm^{-1}$ , and those of MS– $H_2O$  and MS– $(H_2O)_2$  appear at  $30\,192$  and  $30\,241\,cm^{-1}$ , respectively. The assignments of the cluster bands were made on the basis of their FDIR spectra shown later. Vibronic bands that are attributed to the  $n \geq 3$  cluster were not observed. The absence of the higher clusters may be due to their poor fluorescence quantum yield.

Parts b and c of Figure 1 show fluorescence excitation spectra of MS clusters with solvent molecules such as methanol and ammonia, respectively. The  $S_1-S_0$  transition energies of bare MS and these clusters are listed in Table 1. As seen in the table, the shifts of the band origins show characteristic behavior depending on the solvent molecules. The cluster formation with water and methanol causes a blue shift of the transition from the monomer band, while the band of the cluster with ammonia shows a red shift. On the basis of these spectral features, structural difference is expected between the former and the latter clusters;<sup>13</sup> that is, MS would act as a proton acceptor in the former clusters and a proton donor in the latter.

**Infrared Spectra of MS and Its Hydrogen-Bonded Clusters.** The FDIR spectra of the MS monomer and MS– $(H_2O)_n$  ( $n = 1$  and  $2$ ) are shown in Figure 2. These spectra were observed by monitoring the fluorescence due to the excitation

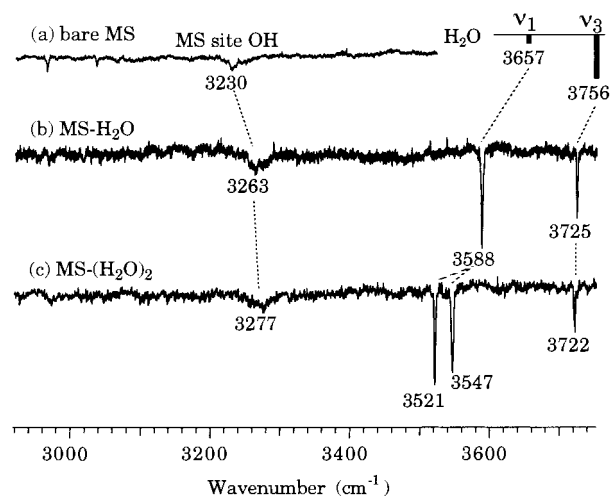


**Figure 2.** Fluorescence-detected infrared (FDIR) spectra of (a) bare MS, (b) MS– $H_2O$ , and (c) MS– $(H_2O)_2$ . The vibrational band positions of bare water are also schematically shown.

of the  $S_1-S_0$  band origin of each species. In the spectrum of bare MS (Figure 2a), a weak band appears at  $3230\,cm^{-1}$  which is uniquely assigned as the absorption due to the OH stretch. The observed frequency is close to those reported in the previous measurements of the IR spectrum in the gas phase ( $3255\,cm^{-1}$ )<sup>14</sup> and the dispersed fluorescence spectrum ( $3220\,cm^{-1}$ ) in a jet.<sup>4</sup> Since typical vibrational frequencies of free OH stretch bands are observed around  $3600\,cm^{-1}$ , the extremely low-frequency OH band observed for bare MS indicates that the intramolecular hydrogen bond is formed. In bare MS, two weak bands are also observed in the CH stretching region (at  $2964$  and  $3035\,cm^{-1}$ ). On the basis of infrared absorption spectrum in the gas phase,<sup>14</sup> these bands are assigned to CH vibrations of the alkoxy and of the phenyl group, respectively. The intensity of the intramolecular hydrogen-bonded OH stretch band is as weak as that of the CH stretches, being in a sharp contrast to a remarkable intensity enhancement due to the intermolecular hydrogen-bond formation, as typically seen in phenol clusters.<sup>12,15</sup> Such a weak intensity of OH stretch vibration has also been found in tropolone, which exhibits a characteristic feature of the OH band involving intramolecular hydrogen bonds in isolated molecules.<sup>8–10</sup>

The infrared spectrum of MS– $H_2O$  is shown in Figure 2b. A weak band appears at  $3263\,cm^{-1}$ , which is blue-shifted by  $30\,cm^{-1}$  from bare MS. The band feature is very similar to the OH stretch of the monomer with respect to the band position, intensity, and width. Therefore, it is readily assigned to the OH stretch of the MS site. Two intense bands appear at  $3725$  and  $3588\,cm^{-1}$ , and they are attributed to the asymmetric ( $\nu_3$ ) and symmetric ( $\nu_1$ ) OH stretches of the water site, respectively.<sup>16</sup> The  $\nu_1$  band in the spectrum shows a distinct intensity enhancement compared to that of the free molecule of water. This drastic increase of the  $\nu_1$  band is characteristic of the hydrogen-bonded clusters in which a water molecule act as a proton donor.<sup>8–10,12,15</sup>

Figure 2c is the infrared spectrum of MS– $(H_2O)_2$ , showing features similar to that of MS– $H_2O$ . A weak band is observed at  $3277\,cm^{-1}$  and is attributed to the OH stretch of the MS site. The band frequency shows a further blue shift from that of MS– $H_2O$ , but the intensity is not enhanced so much. Three intense bands of the water site appear in the higher frequency region. Because of the similarity with the spectrum of MS– $H_2O$ , the bands at  $3547$  and  $3521\,cm^{-1}$  are attributed to  $\nu_1$ . The band at  $3722\,cm^{-1}$  is assigned to two overlapped  $\nu_3$  bands. Such

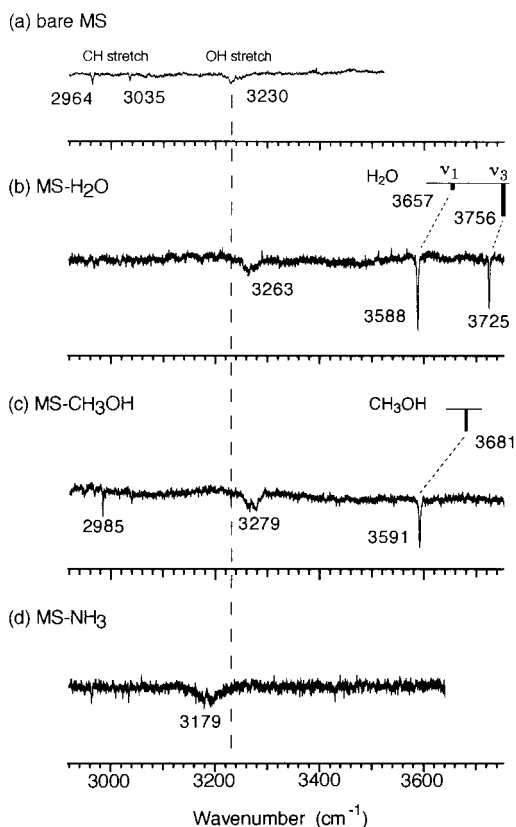


**Figure 3.** FDIR spectra of (a) bare MS, (b) MS–H<sub>2</sub>O, (c) MS–CH<sub>3</sub>OH, and (d) MS–NH<sub>3</sub>.

overlap of the  $\nu_3$  bands was also found for tropolone–water and phenol–water clusters.<sup>8,10,12,15</sup>

The infrared spectra of the MS–CH<sub>3</sub>OH and –NH<sub>3</sub> clusters are shown in Figure 3 in comparison with those of bare MS and MS–H<sub>2</sub>O. In the spectrum of MS–CH<sub>3</sub>OH shown in Figure 3c, a weak and broad band appearing at 3279 cm<sup>-1</sup> is immediately assigned to the OH stretch band of the MS site showing a blue shift of about 40 cm<sup>-1</sup> compared to that of bare MS. Similar to MS–(H<sub>2</sub>O)<sub>n</sub>, the intensity of the band is not enhanced so much. A sharp and intense band is observed at 3591 cm<sup>-1</sup>, which is uniquely assigned to the OH stretch of the methanol site. The band frequency is red-shifted by about 90 cm<sup>-1</sup> from that of free methanol,<sup>16</sup> suggesting the cluster structure in which methanol acts as a proton donor to MS. It is noted, thus, that the spectrum of MS–CH<sub>3</sub>OH is very similar to that of MS–H<sub>2</sub>O, except for the free OH band. The weak but sharp band observed at 2985 cm<sup>-1</sup> should be assigned to the CH stretching band of the alkoxy group in MS or the methanol site. Both of free MS and methanol show the CH stretch in this region.<sup>14,16</sup>

Figure 3d is the infrared spectrum of MS–NH<sub>3</sub>. The OH vibrational band of the MS site appears at 3179 cm<sup>-1</sup>, showing a red shift from the MS monomer. This red shift is quite contrary to the feature of the clusters with water or methanol. The intensity of the band is also weak, and the bandwidth becomes wider. Two very weak bands are observed in the CH stretch region. They are the similar bands as the CH bands of bare MS. Though NH stretches are expected in 3300–3400 cm<sup>-1</sup> region, no band was found in this region.

## Discussion

**Intramolecular Hydrogen Bond in MS.** The main aim of this study is to observe solvation effects on the intramolecular

hydrogen bond of MS. The evidence for the intramolecular hydrogen bond between the hydroxyl and carbonyl groups of MS can be seen in the infrared spectra of the OH stretch band, that is, the remarkable low-frequency shift and the intensity reduction. As was demonstrated in the hydrogen-bonded clusters of tropolone, the breakdown of the intramolecular hydrogen bond due to the microsolvation may cause a drastic change of the OH stretch band, such as a blue shift in frequency and an enhancement in intensity.<sup>8</sup>

As shown in Figures 2 and 3, it is evident that the OH bands of the MS site in MS–(H<sub>2</sub>O)<sub>n</sub> ( $n = 1$  and 2), –CH<sub>3</sub>OH, and –NH<sub>3</sub> are very similar to the monomer. Such a conservation of the characteristics of the OH stretch band suggests that the intramolecular hydrogen bond is still retained in these clusters despite the microsolvation.

Previous study of solvation of the intramolecular hydrogen bond in tropolone suggested that the breakdown of the intramolecular hydrogen bond occurs when the proton affinity (PA) of the solvent exceeds a critical value.<sup>8</sup> In the case of tropolone, the critical value of PA was estimated about 200–220 kcal/mol. The PA of H<sub>2</sub>O, (H<sub>2</sub>O)<sub>2</sub>, CH<sub>3</sub>OH, and NH<sub>3</sub> are 167, 201, 182, and 204 kcal/mol, respectively.<sup>17–19</sup> The PA of (H<sub>2</sub>O)<sub>2</sub> and NH<sub>3</sub> are close to the critical value for tropolone. On the other hand, the acid dissociation constant, p*K*<sub>a</sub>, of MS is 10.2, and the acidity of MS is much weaker than that of tropolone (p*K*<sub>a</sub> = 6.7).<sup>7,11</sup> The results indicate that the proton donation to solvent molecules is less favorable for MS, and the clusterization with compounds of much higher PA (or higher size of cluster) is required for the intramolecular hydrogen bond of MS to be broken.

### Structure of the MS–Solvent Hydrogen-Bonded Clusters.

**The 1:1 Clusters.** In this section, we discuss the cluster structures based on the observed spectra. As for the structure of MS–H<sub>2</sub>O, the following data were obtained in this study: (i) The OH band of the MS site exhibits a slight blue shift from that of monomer, and its intensity and band shape do not change by the cluster formation. (ii) The symmetric OH stretch of the water site ( $\nu_1$ ) shows a red shift and its intensity is largely enhanced, while there is no drastic change in the antisymmetric OH stretch ( $\nu_3$ ). (iii) The band origin of the S<sub>1</sub>–S<sub>0</sub> transition shows a blue shift upon the cluster formation.

The first result means that the intramolecular hydrogen bond is preserved in the cluster. The second indicates that the one of the OH oscillators of the water acts as the proton donor of the intermolecular hydrogen bond and that the other oscillator is free from hydrogen-bond formation. For the third result, it is well-known that a ( $\pi$ ,  $\pi^*$ ) transition of aromatic molecules shows a blue shift when the molecule acts as a proton acceptor<sup>13</sup> and that the S<sub>1</sub>–S<sub>0</sub> transition of MS is assigned to the ( $\pi$ ,  $\pi^*$ ) transition.<sup>3</sup> Thus, the third result represents the cluster structure in which MS acts as the proton acceptor in the intermolecular hydrogen bond.

Being subjected to the requirements described above, two cluster structures are suggested: (a) a hydroxyl group of the water site is bonded to the carbonyl group of MS (type a); (b) a hydroxyl group of the water site attaches to the hydroxyl group of MS (type b).<sup>20</sup> The ab initio calculated structures of these two isomers are shown in Figure 4, a and b, respectively. The details of the calculation are described later. Similar cluster structures have been proposed by Zwier and co-workers for tropolone–H<sub>2</sub>O, in which the intramolecular hydrogen bond between the carbonyl and hydroxyl groups is solvated by a water molecule.<sup>9,10</sup>

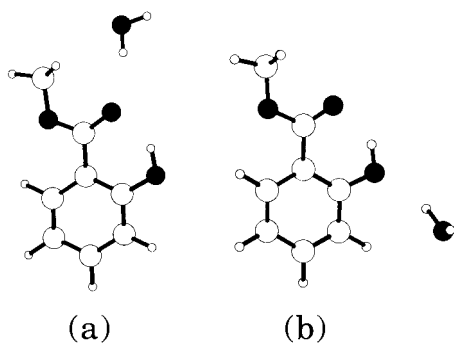


**Figure 4.** Ab initio structures of MS–H<sub>2</sub>O. The calculation level is HF-SCF/6-31G(d,p).

Different frequency shifts are expected for the intramolecular hydrogen-bonded OH in these two isomers from the standpoint of chemical intuition. In isomer **a**, the intermolecular hydrogen-bond formation to the carbonyl group of MS reduces the negative charge density of the oxygen molecule of the carbonyl group, so that the intramolecular hydrogen bond will be weakened, resulting in a blue shift of the OH stretch frequency of the MS site. In the case of isomer **b**, on the other hand, the intermolecular hydrogen bond to the hydroxyl group of MS reduces the negative charge density on the oxygen molecule of the hydroxyl group, and it may weaken the OH bond of MS, resulting in a red shift of the OH stretch frequency. Such a phenomenon has been known in condensed-phase infrared studies as the cooperative strengthening of the intramolecular hydrogen bond by the presence of the intermolecular hydrogen bond.<sup>21,22</sup> The observed blue shift of the OH stretch frequency of the MS site in MS–H<sub>2</sub>O, as shown in Figures 2 and 3, therefore suggests that the type **a** structure is favorable for MS–H<sub>2</sub>O.

To confirm the above qualitative discussion, we performed ab initio molecular orbital calculations by using the Gaussian 94 program package.<sup>23</sup> The calculation level was HF-SCF/6-31G(d,p), and minimum-energy structures and their harmonic vibrational frequencies were computed. To find possible isomers of MS–H<sub>2</sub>O, several trials of the initial geometry were attempted. We found two stable forms of MS–H<sub>2</sub>O corresponding to the isomers, as shown in Figure 4.<sup>24</sup> In both isomers, the water molecule donates the hydrogen to (a) the carbonyl group or (b) the hydroxyl group of the MS site.

The stabilization energies for the two isomers are almost the same (3.669 and 3.185 kcal/mol for isomers **a** and **b**, respectively, including the zero-point energy corrections), and it is hard to discriminate one of the candidates from the energy difference obtained with this calculation level. Calculated OH and CH stretching vibrational frequencies of the two isomers are listed in Table 2. Since we used the Hartree–Fock

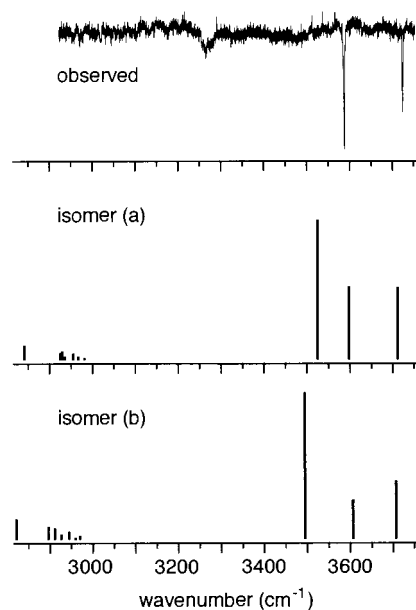


**Figure 5.** Comparison between (upper) the observed and (lower) simulated infrared spectra of MS–H<sub>2</sub>O. The latter spectra are based on the HF-SCF/6-31G(d,p) level ab initio calculations, and spectra **a** and **b** correspond to isomer **a** and **b** in Figure 4, respectively. As for the band positions in the simulated spectra, the scaling factors (0.8751 and 0.8735 for isomer **a** and **b**, respectively) are applied to the frequencies shown in Table 2.

approximation, the calculated vibrational frequencies are about 10% higher than the observed frequencies. Comparison between the observed and calculated infrared spectra is shown in Figure 5, in which the calculated vibrational frequencies are scaled by the factor 0.8751 and 0.8735 for isomer **a** and **b**, respectively. The simulated spectra poorly reproduce the frequency and intensity of the OH stretch of the MS site, while those of the water site agree rather well with the observed. It has been reported that the simulation of infrared spectra of intramolecular hydrogen-bonded OH by ab initio calculations is not straightforward.<sup>10,11</sup> Their red shifts tend to be underestimated while the intensities are generally overestimated. However, it is worthwhile to note that the present calculated frequency of the OH stretching vibration of the MS site shows the *blue* shift by 20 cm<sup>−1</sup> for isomer **a** upon the hydrogen bond formation, while that of isomer **b** is *red*-shifted by 20 cm<sup>−1</sup>. This tendency agrees with that expected in the above qualitative discussion, supporting the preference of isomer **a**.

Electronic and infrared spectral features of MS–CH<sub>3</sub>OH are quite similar to those of MS–H<sub>2</sub>O: In the electronic transition, the band origin of MS–CH<sub>3</sub>OH shows the blue shift, and the amount of the shift is also close to that of MS–H<sub>2</sub>O. In the infrared spectrum, the band positions and intensities of observed

**TABLE 2: Infrared Frequencies (cm<sup>−1</sup>) and Intensities (km mol<sup>−1</sup>) of MS–H<sub>2</sub>O in the OH and CH Stretching Region**

bare MS			MS–H <sub>2</sub> O(isomer <b>a</b> )		MS–H <sub>2</sub> O(isomer <b>b</b> )		obsd freq	assignment
calcd <sup>a</sup> freq	int	obsd freq	calcd <sup>a</sup> freq	int	calcd <sup>a</sup> freq	int		
3229.3	43.8	2964	3241.3	34.1	3229.5	43.3	methyl CH str	
3315.2	27.0		3337.2	16.3	3315.3	26.5	methyl CH str	
3332.0	23.5		3343.5	20.3	3332.5	22.9	methyl CH str	
3348.4	8.1		3349.8	8.0	3350.2	9.1	phenyl CH str	
3370.6	16.2		3372.1	15.3	3371.8	15.1	phenyl CH str	
3384.9	9.1		3385.7	8.5	3388.5	1.3	phenyl CH str	
3399.4	5.6	3230	3401.5	5.0	3399.7	6.0	phenyl CH str	
4007.8	293.7		4028.4	324.2	3999.6	330.5	OH str	
			4113.2	169.9	4128.4	86.4	3263	water $\nu_1$
			4243.1	168.3	4243.1	129.1	3588	water $\nu_3$

<sup>a</sup> The calculation level is HF-SCF/6-31G(d,p).

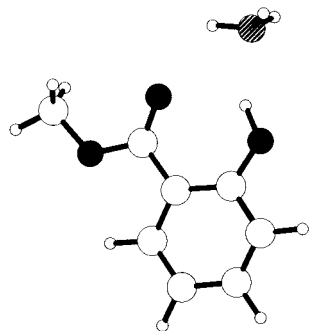


**Figure 6.** Ab initio structures of MS-NH<sub>3</sub>. The calculation level is HF-SCF/6-31G.

OH stretching bands resemble the spectrum of MS-H<sub>2</sub>O, except for the absence of the free OH ( $\nu_3$ ) band in the MS-H<sub>2</sub>O. In particular, the OH stretching band of MS site shows a blue shift, corresponding to that of MS-H<sub>2</sub>O. On the basis of the discussion on MS-H<sub>2</sub>O, it is expected that MS-CH<sub>3</sub>OH has a structure similar to isomer **a** of MS-H<sub>2</sub>O in Figure 4.

In contrast, the spectral features of MS-NH<sub>3</sub> are very different from those of MS-H<sub>2</sub>O or -CH<sub>3</sub>OH with respect to the following: (i) The OH stretch of the MS site shows a red shift of 51 cm<sup>-1</sup>. (ii) No strong infrared absorption was found for the NH<sub>3</sub> site. (iii) The band origin of the S<sub>1</sub>-S<sub>0</sub> transition exhibits a red shift of 17 cm<sup>-1</sup>.

All the features are opposite to those of other clusters studies here and suggest a different structure for MS-NH<sub>3</sub> from the others. These features are well understood with the structure in which MS donates the proton to NH<sub>3</sub>, as is shown in Figure 6, being the intramolecular hydrogen bond still remained. The intermolecular hydrogen-bond formation with NH<sub>3</sub>, in addition to the intramolecular hydrogen bond, weakens the OH bond, leading to a further red shift of the OH band of the MS site. The second datum is consistent with the well-known fact that the infrared absorption intensity of the proton acceptor site does not show enhancement. In addition, the red shift of the electronic transition is also a favorable feature of the proton donor site.

The presence of the neighboring carbonyl group prohibits the linear O-H...N configuration, which is favorable for the ordinary intermolecular proton donation. However, the proton affinity of ammonia is 208.3 kcal/mol and is much larger than that of water or methanol (165 and 185 kcal/mol, respectively).<sup>17-19</sup> Such a large PA would offset the steric disadvantage of the structure. The low-level ab initio calculation (HF-SCF/6-31G) also shows the potential minimum for the structure shown in Figure 6 and supports the above discussion.

**The Structure of MS-(H<sub>2</sub>O)<sub>2</sub>.** The infrared and electronic spectra of MS-(H<sub>2</sub>O)<sub>2</sub> show the following features: (i) The OH stretch of the MS site appears at 3277 cm<sup>-1</sup>. Its frequency is similar to that of MS and MS-H<sub>2</sub>O, but slightly blue-shifted, 47 and 14 cm<sup>-1</sup> from bare MS and MS-H<sub>2</sub>O, respectively. The intensity of the band is much weaker than the intermolecular hydrogen-bonded OH of the water site. (ii) The intermolecular hydrogen-bonded OH stretches of the water site are found at 3521 and 3547 cm<sup>-1</sup>. Both are red-shifted from the corresponding band of MS-H<sub>2</sub>O. (iii) A free OH appears at 3722 cm<sup>-1</sup>, which is almost the same as the free OH band of MS-H<sub>2</sub>O. (iv) The band origin of the S<sub>1</sub>-S<sub>0</sub> transition is 186 cm<sup>-1</sup> blue-shifted from that of bare MS, while the blue shift of MS-H<sub>2</sub>O is 137 cm<sup>-1</sup>. (Addition of the one more water induces only a 49 cm<sup>-1</sup> shift.)

All the spectral features indicate that the intramolecular hydrogen bond is still preserved in the cluster, and MS acts as

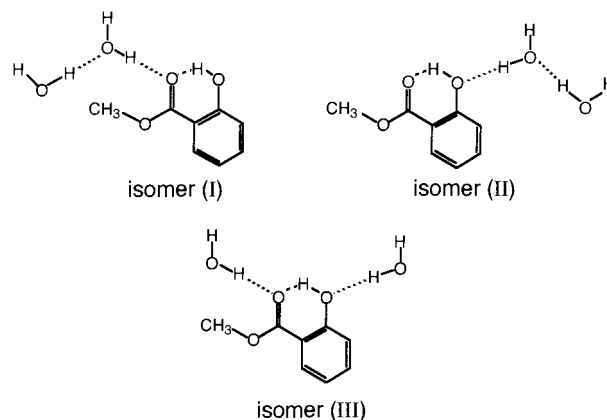


**Figure 7.** Schematic representation of the possible structures of MS-(H<sub>2</sub>O)<sub>2</sub>.

a proton acceptor in MS-(H<sub>2</sub>O)<sub>2</sub>, as well as MS-H<sub>2</sub>O and -CH<sub>3</sub>OH. Based on the feasible structures of MS-H<sub>2</sub>O, several candidates of the structure of MS-(H<sub>2</sub>O)<sub>2</sub> are schematically given in Figure 7. Isomers **I** and **II** are the extended forms of isomers **a** and **b** of MS-H<sub>2</sub>O, respectively, and isomer **III** is a hybrid type of the former two. In each case, two hydrogen-bonded OH of the water site are expected around 3500-3600 cm<sup>-1</sup>, while two free OH of the water site should be almost degenerate at around 3720 cm<sup>-1</sup>.

The first datum is a key for the structure determination. The OH stretch of the MS site shows a further blue shift than that of MS-H<sub>2</sub>O. Such an effect is expected only in isomer **I**. This is because, as was discussed for MS-H<sub>2</sub>O, the hydrogen-bond formation onto the hydroxyl group of MS causes the red shift of its frequency. Therefore, isomer **I** in Figure 7 is considered to be the most probable form for MS-(H<sub>2</sub>O)<sub>2</sub>.

## Conclusion

In this study, we observed the S<sub>1</sub>-S<sub>0</sub> fluorescence excitation and fluorescence-detected infrared spectra of MS-(H<sub>2</sub>O)<sub>n</sub> ( $n = 1$  and 2), -CH<sub>3</sub>OH, and -NH<sub>3</sub>. It was shown that every cluster holds the intramolecular hydrogen bond, though the bond is more or less perturbed by the intermolecular hydrogen-bond formation with the solvent molecules. A breakdown of the intramolecular bond with microsolvation was not found in these small-size MS clusters, while complete transformation from an intra- to intermolecular hydrogen bond was observed in tropolone. This corresponds to a much lower acidity of MS ( $pK_a = 10.2$ ) than tropolone ( $pK_a = 6.7$ ) in the condensed phase. In the case of MS, the intramolecular hydrogen bond is formed between the neighboring hydroxyl and carbonyl groups, which are very close to each other. Therefore, it is difficult to insert a solvent molecule between these two groups. This steric factor might protect the intramolecular hydrogen bond of MS.

## References and Notes

- (1) Klöpffer, W.; Kaufmann, G. *J. Lumin.* **1979**, *20*, 283.
- (2) Heimbrook, L. A.; Kenny, J. E.; Kohler, B. E.; Scott, G. W. *J. Chem. Phys.* **1981**, *75*, 5201.
- (3) Heimbrook, L. A.; Kenny, J. E.; Kohler, B. E.; Scott, G. W. *J. Phys. Chem.* **1983**, *87*, 280.
- (4) Felker, P. M.; Lambert, W. R.; Zewail, A. H. *J. Chem. Phys.* **1982**, *77*, 1603.
- (5) Kuper, J. W.; Perry, D. S. *J. Chem. Phys.* **1984**, *80*, 4640.
- (6) Herek, J. L.; Pedersen, S.; Bañares, L.; Zewail, A. H. *J. Chem. Phys.* **1992**, *97*, 9046.
- (7) Tanaka, M. *The Acid and Base*, 2nd ed.; Shokabou: Tokyo, 1981.
- (8) Mitsuzuka, A.; Fujii, A.; Ebata, T.; Mikami, N. *J. Chem. Phys.* **1996**, *105*, 2618.

- (9) Frost, R. K.; Hagemester, F.; Arrington, C. A.; Schleppenbach, D.; Zwier, T. S.; Jordan, K. D. *J. Chem. Phys.* **1996**, *105*, 2595.
- (10) Frost, R. K.; Hagemester, F.; Arrington, C. A.; Zwier, T. S.; Jordan, K. D. *J. Chem. Phys.* **1996**, *105*, 2605.
- (11) Bréf eret, E. F.; Martin, M. M. *J. Lumin.* **1978**, *17*, 49.
- (12) Ebata, T.; Fujii, A.; Mikami, N. *Int. Rev. Phys. Chem.*, in press, and references therein.
- (13) For example: Abe, H.; Mikami, N.; Ito, M. *J. Phys. Chem.* **1982**, *86*, 1768.
- (14) Wójcik, M. J.; Paluszkiwicz, C. *Can. J. Chem.* **1983**, *61*, 1449.
- (15) Watanabe, T.; Ebata, T.; Tanabe, S.; Mikami, N. *J. Chem. Phys.* **1996**, *105*, 408.
- (16) Herzberg, G. *Molecular Spectra and Molecular Structure II. Infrared and Raman Spectra of Polyatomic Molecules*; Van Nostrand Reinhold: New York, 1945.
- (17) Lias, S. G.; Liebman, J. F.; Levin, R. D. *J. Phys. Chem. Ref. Data* **1984**, *13*, 695.
- (18) Canningham, A. J.; Payzant, J. D.; Kebarle, P. *J. Am. Chem. Soc.* **1972**, *94*, 7627.
- (19) Meot-Ner (Mautner), M.; Sieck, L. W. *J. Am. Chem. Soc.* **1991**, *113*, 4448.
- (20) Another structure is also possible; a hydroxyl group of the water molecule forms a ring with the hydroxyl and carbonyl groups of MS ("ring"

type). However, this "ring" type structure seems to be less favorable for MS-H<sub>2</sub>O than the "exterior" structures shown in Figure 4, because the distance between the carbonyl and hydroxyl groups of the MS molecule is too short to insert one more hydroxyl group of the water molecule. In fact, the "ring" structure of MS-H<sub>2</sub>O does not have a potential minimum in our ab initio calculation (see text).

- (21) Spencer, J. N.; Heckman, R. A.; Harner, R. S.; Shoop, S. L.; Robertson, K. S. *J. Phys. Chem.* **1973**, *77*, 3103.
- (22) Spencer, J. N.; Robertson, K. S.; Quick, E. E. *J. Phys. Chem.* **1974**, *78*, 2236.
- (23) Frisch, M. J.; Trucks, G. W.; Schlegel, H. B.; Gill, P. M. W.; Johnson, B. G.; Robb, M. A.; Cheeseman, J. R.; Keith, T.; Petersson, G. A.; Montgomery, J. A.; Raghavachari, K.; Al-Laham, M. A.; Zakrzewski, V. G.; Ortiz, J. V.; Foresman, J. B.; Cioslowski, J.; Stefanov, B. B.; Nanayakkara, A.; Challacombe, M.; Peng, C. Y.; Ayala, P. Y.; Chen, W.; Wong, M. W.; Andres, J. L.; Replogle, E. S.; Gomperts, R.; Martin, R. L.; Fox, D. J.; Binkley, J. S.; Defrees, D. J.; Baker, J.; Stewart, J. P.; Head-Gordon, M.; Gonzalez, C.; Pople, J. A. *Gaussian 94*, Revision D.4; Gaussian, Inc.: Pittsburgh, PA, 1995.
- (24) These ab initio structures are visualized by using *MOLCAT*, ver. 2.5: Tsutui, Y.; Wasada, H. *Chem. Lett.* **1995**, 517.